

L. Zill

THE GROUND MAGNETIC METHOD
IN GEOTHERMAL EXPLORATION

Camilo P. Ignacio*
UNU Geothermal Training Programme
National Energy Authority
Grensasvegur 9, 108 Reykjavik
ICELAND

*
Permanent address:
PNOC Energy Development Corporation
Geothermal Division
Merritt Road
Fort Bonifacio, Metro Manila
PHILIPPINES

ABSTRACT

An outline is presented of the principles and applications of the ground magnetic methods in geothermal exploration. An example is included of the use of a ground magnetic survey for sub-surface structural mapping in a low temperature area in Sumarlidabaer in S-Iceland. The total magnetic field intensity in the Sumarlidabaer geothermal area was measured with a proton precession magnetometer. The measurements were made every 5 m along 21 profile lines each some 300 m long with a spacing of 20 m between the lines. Several linear anomalies of some 1000 gammas were found, which are caused by dykes and faults. These structures are very likely the main flow channels of the geothermal water in the area. The magnetic anomalies were interpreted by a dyke and semi-infinite block models, in order to locate the faults and dykes precisely on the surface. The warm springs are very likely associated with one of the faults.

TABLE OF CONTENTS

	<u>Page</u>
ABSTRACT	3
1 INTRODUCTION	
1.1 Scope of work	7
2 THE MAGNETIC METHOD	
2.1 Introduction	8
2.1.1 The simple magnet	9
2.1.2 The earth's magnetic field	10
2.2 Magnetic data processing	13
2.2.1 Survey data reduction	13
2.2.2 Numerical filter processing	13
2.3 Ground magnetic field measurements	15
2.4 Instrumentation	15
2.5 Interpretation of magnetic field data	16
2.5.1 The dyke model	17
2.5.2 Interpretation by characteristics	20
2.5.3 Computer model interpretation	26
3 GROUND MAGNETIC SURVEY AT SUMARLIDABAER, S-ICELAND	
3.1 Introduction	28
3.2 Geology of the study area	28
3.3 Magnetic measurements and data processing	30
3.4 Interpretation of the magnetic anomalies	32
3.4.1 Assumptions and guidelines to interpretation	34
3.4.2 Methods of interpretation	35
3.4.3 Summary of the results	42
3.5 Conclusions	43
ACKNOWLEDGEMENTS.....	45
REFERENCES	46

LIST OF FIGURES

	<u>Page</u>
2.1 The magnetic dipole	10
2.2 The magnetic vector	11
2.3 The magnetic anomaly, ΔF	12
2.4 The dyke model	18
2.5 The semi-infinite block model	19
2.6 Normalized standard curves for magnetic anomalies due to dykes	21
2.7 Maximum and half-maximum slopes superimposed on a linear, regional field	22
2.8 Definition of symbols and lengths used in the interpretation charts	23
2.9 Interpretation charts used for determining dyke parameters (b/d and) for: (a)-(c)dyke, (d)semi-infinite block models	24
2.10 Charts for making depth estimates	25
2.11 Dyke model computed from the HALLI program	27
3.1 Ground magnetic survey at Sumarlidabaer	31
3.2 Total magnetic intensity map	33
3.3 Interpreted dyke and fault model	37
3.4 Top of the reversely magnetised dyke	38
3.5 Interpreted 2-dimensional model along line-00	39
3.6 Interpreted 2-dimensional model along line-260 ...	40
3.7 Interpreted 2-dimensional model along line-260 using different parameters	41

LIST OF TABLES

1: Estimated parameters for the reversely magnetised dyke	36
--	----

1 INTRODUCTION

1.1 Scope of work

This report is a part of the work of the author undertaken during 6 months training in geophysical exploration methods held from April to October 1982 at the UNU Geothermal Training Programme, National Energy Authority in Reykjavik, Iceland.

The training started with a 4-week lecture series covering the general aspects of geothermal energy exploration, utilisation, planning and management. This was followed by site visits to the various places in Iceland, where geothermal energy is being developed and utilized. The rest of the training period was devoted to the study on the application of various geophysical exploration methods. For the DC-resistivity method, 3 weeks were spent on the Schlumberger profiling, vertical electrical soundings and the "head-on" profiling resistivity techniques. One week was spent on the practical aspects of gravity surveying and another week on field work in magnetotellurics. One week was spent in borehole geophysics at the Krafla geothermal field. The author also received tuition in computer interpretation techniques for magnetic, gravity and resistivity data. Seven weeks were devoted to the study of the interpretation methods of ground magnetic data and the writing of this report.

2 MAGNETIC METHODS

2.1 Introduction

Aeromagnetic and ground magnetic surveys are used in geothermal exploration to map subsurface structural features, and as an aid to geological mapping where outcrops are scarce. The purpose of magnetic surveys is to detect rocks or minerals possessing contrasting magnetic properties, which reveal themselves by causing disturbances or anomalies in the intensity of the Earth's magnetic field. In some high-temperature geothermal areas, a good correlation is found between altered ground and the reduced intensity of magnetisation caused by the alteration of magnetic minerals (Palmasson, 1975). Sometimes aeromagnetic surveys are used as a reconnaissance tool in selecting prospect areas for more detailed exploratory work. Ground magnetic surveys are often done as a complement to other geophysical methods and geological mapping, particularly in order to detect vertical structures.

In most high temperature geothermal areas, determination of the heat source is a major concern in geophysical exploration. A recent application of the magnetic method tackles this particular problem by mapping the Curie point isothermal surface, below which the rocks are non-magnetic. The process involves the computation of the bottom of the magnetised crust from the spectral analysis of the residual magnetic anomalies (Bhattacharyya and Leu, 1975), reduced to the pole.

In the low temperature geothermal fields of Iceland, ground magnetics are extensively used for tracing hidden dykes and faults that often control the flow of thermal water to the surface (Bjornsson, 1981; Flovenz and Georgsson, 1982). The method is considered to be the cheapest of the various other geophysical methods and also the easiest to perform.

2.1.1 The simple magnet

A magnet has always two poles, a north and a south pole, also referred to as a positive and a negative pole. Such a magnet creates a field of force around itself, with the geometry of the typical dipole field. The lines of force go from the positive to the negative pole, defined positive in this direction.

A single hypothetical magnetic pole, or in practical terms the end of a long magnet whose far end is distant, creates at a distance r a radial force field whose strength is

$$F = m/r^2 \quad (2.1)$$

where m is the strength of the pole.

Let us consider a magnet, where the distance between the opposite poles is l , and their strength m . It can be shown, by combining the effect from both poles, that the force at a distance r from the magnet is

$$\begin{aligned} F_{\parallel}(\phi, r) &= 2M \cos \phi / r^3 \\ F_{\perp}(\phi, r) &= M \sin \phi / r^3 \end{aligned} \quad (2.2)$$

These two components are parallel and perpendicular to the direction of the magnet (Fig. 2.1). M is called the magnetic moment, defined as $M = l \times m$.

This simple derivation of the magnetic field serves to demonstrate some of its basic properties. It can be seen that along a line of constant direction from the magnet, the force diminishes with the distance cubed. It is interesting to compare this with the gravity effect which diminishes with the distance squared. This manifests itself as a marked difference in the nature of the Earth's anomalous magnetic and gravity fields.

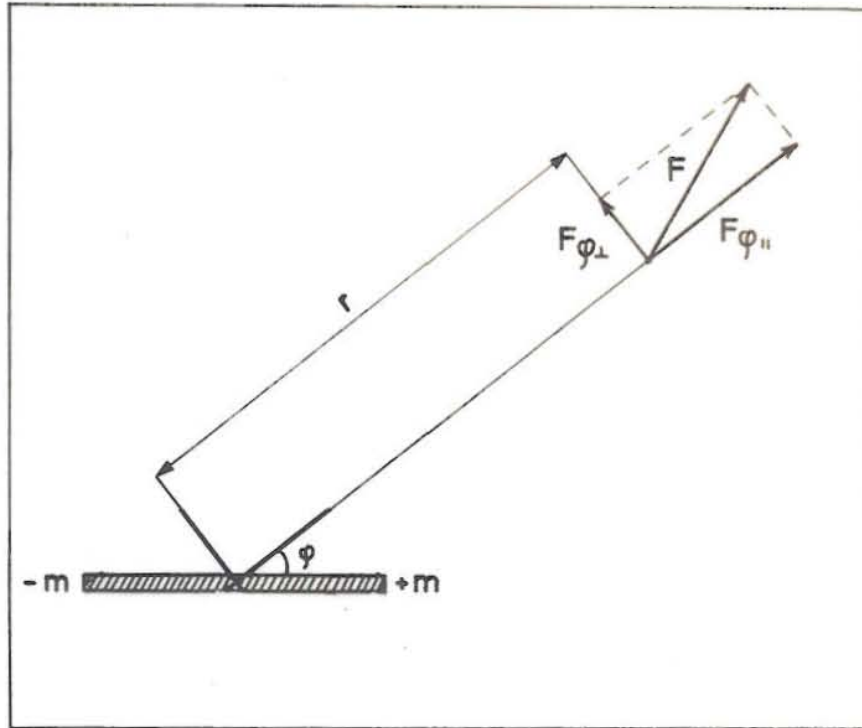


Fig. 2.1 The magnetic dipole.

2.1.2 The Earth's magnetic field

The Earth's field can be represented to a close approximation as the field of a dipole, situated at a center of the Earth with its magnetic moment pointing to the geographical south pole. The lines of force intersect the Earth's surface in such a way that they point upwards at the southern magnetic pole, change to being horizontal and north pointing at the magnetic meridian and again to vertical downward pointing to the magnetic north pole.

Superimposed on the Earth's normal field is the anomalous field caused by variations in the magnetisation of the upper crust. Only this part of the field is of interest in magnetic prospecting, as it reflects the shallow geological targets. The magnitude of the Earth's field is typically about 50,000 gammas (nT, nano Tesla), whereas the amplitude of the anomalies can only reach a few thousand gammas, and is usually much less. Thus the normal field is usually dominant.

The magnetic force field as measured at any point on the Earth's surface has the property of both direction and magnitude. This force may be resolved into a vertical component Z and a horizontal component H . The horizontal component may be further resolved into a northerly component X and an easterly component Y . The vector is also commonly defined by the polar coordinates, inclination (I), declination (D) and magnitude (Fig. 2.2).

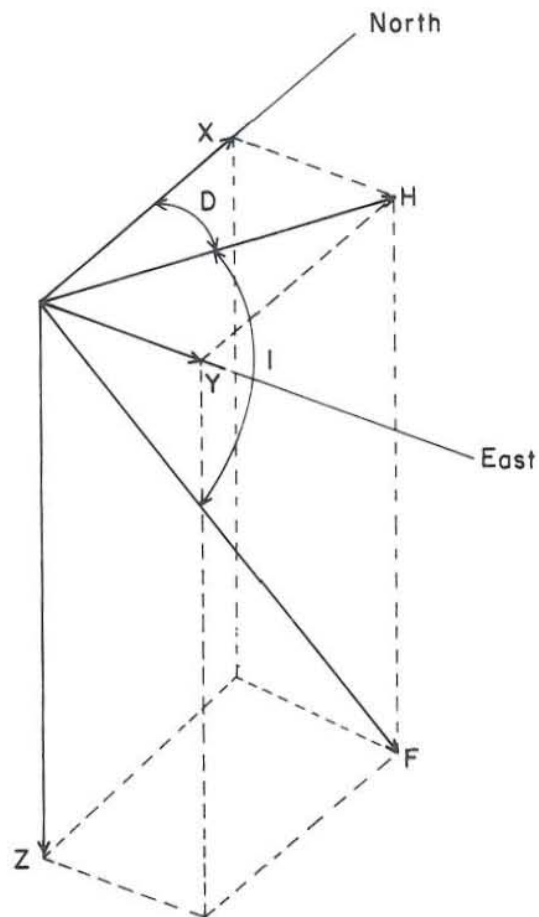


Fig. 2.2 The magnetic vector.

We assume that the Earth's magnetic field is uniform over a limited area, and defined by a vector \vec{F}_0 . A disturbing magnetic source nearby, would give at a point P, an additional magnetic field vector, $\Delta\vec{F}^1$. The total magnetic field at P, is then defined as

$$\vec{F}_1 = \vec{F}_0 + \Delta\vec{F}^1 \quad (2.2)$$

In field surveys when the "total field" instruments are used, one actually measures the total magnetic field intensity. The difference between the magnitude of the normal magnetic force \vec{F}_0 and the total magnetic force \vec{F}_1 is called the magnetic anomaly ΔF . Hence,

$$\Delta F = |\vec{F}_1| - |\vec{F}_0| \quad (2.3)$$

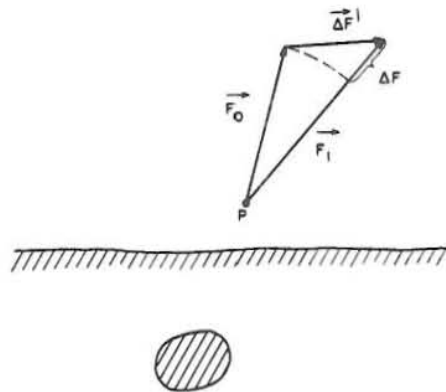


Fig. 2.3 The magnetic anomaly, ΔF .

Note that the magnitude of the anomaly measured is not the same as that of the anomalous field vector $\Delta\vec{F}^1$. In quantitative interpretation, the anomaly is by necessity assumed to be equal to the projection of the anomalous vector onto the direction of the normal field, \vec{F}_0 . This assumption is valid approximately as $\Delta\vec{F}^1$ is usually much smaller than \vec{F}_0 , and the total field is almost parallel to the normal field \vec{F}_0 . When surveys involve the measurement of definite directional components of the field, this approximation is not relevant, as true magnitudes of the anomalous vector components are obtained.

2.2 Magnetic data processing

2.2.1 Survey data reduction

The data obtained from ground magnetic measurements may require corrections for diurnal and micropulsation time variation (Breiner, 1973). Diurnal variations are monitored at a base station and subtracted from the station readings. In some surveys, where the amplitude of the anomalies are big and well defined, diurnal corrections are unnecessary. Sometimes low-pass filtering is used to remove noise that is disturbing the anomalies of interest. This can either be done by hand, by simple weighted averaging, or by a computer using more advanced filter operators.

When measurements are taken in rugged areas, the effect of terrain should be considered in the interpretation. Gupta and Fitzpatrick (1971) noted that magnetic effects due to the terrain can be as much as 1000 gammas in areas of moderate relief, where the bedrock contains a few percent of magnetite. The correction for terrain effect in entire magnetic maps is in practice problematic and not commonly done. However, anomalies caused by individual features can be simulated and noted.

2.2.2 Numerical filter processing

Often the anomalous field is composed of different types of anomalies, having different widths or frequency contents. Several filtering techniques can be used to enhance one type of anomalies at the expense of others. Typical situations could be when the anomalies of significance are either masked by high frequency noise, or dominated by broad regional anomalies. This type of filtering involves both simple high- or low-pass filtering as well as other mathematical operations which modify the frequency content of the data. It is usually done by convolving an operator

with the gridded numerical expression of the magnetic map. A few of these numerical processing methods will be mentioned here.

The study of magnetic anomalies is complicated because of the variation in the direction of the vector of magnetisation and the Earth's total field. This causes the magnetic anomalies to have asymmetrical shapes, confusing their relations to the magnetic sources. This can sometimes be rectified by digital processing of the data. The numerical calculation in this process is called "reduction to the pole" (Baranov, 1975). The method provides a magnetic map simulating the field which would be observed at the magnetic pole where the field is vertical. Anomalies reduced to the pole have an appearance similar to the gravity anomalies and are therefore easy to visualize. The application to the method is limited by its assumption of a uniform direction of magnetisation of the sources. Thus, if remanent magnetisation of varying direction is present the results are misleading.

Continuation of the magnetic field involves the simulation of the field, at an elevation below or above the level of measurements. The magnetic intensity at the point of observation can be continued upward to higher levels or downward to lower levels near the rocks producing the field. In magnetic maps, where near surface magnetised bodies distort the magnetic field, it is sometimes beneficial to project the field upwards to a level where the anomalies are not disturbed. On the other hand, if the narrow anomalies are so weak that they can hardly be detected then it is necessary to put the measurement downward, to a level where the anomalies are clearly manifested.

The vertical derivatives of the magnetic field are often calculated. This is also a numerical method enhancing narrow anomalies obscured by the regional anomalies. Derivative maps show a prominent steep slope for the

smaller anomalies and are useful to define the boundaries of the magnetised bodies. The second derivative and sometimes the fourth are used for this purpose.

2.3 Ground magnetic field measurements

The procedure for a ground magnetic survey is rather simple and easy as compared for example to a resistivity survey. All that is required is a portable magnetometer and some means to position the observation points (air photos, detailed maps and sometimes a theodolite). The survey is prepared by first choosing a series of profiles normal to the known geologic structures. Then measurements are taken along the profile at intervals of 5 m, or so, depending on the expected wavelength of the anomalies.

In areas where the anomalies are of small amplitude, a base magnetometer is used, in addition to the roving magnetometer, to monitor diurnal variations. During magnetic storms, surveys are discontinued.

2.4 Instrumentation

A total field magnetometer (proton precession) measures the scalar magnitude of the magnetic field. The proton magnetometer is the most widely used instrument for ground magnetic surveys. It has a sensitivity of ± 1 gamma. Its sensor contains a vessel of liquid hydrocarbon and it operates on a principle that the frequency generated by the precessing protons is proportional to the total magnetic field intensity. Inside the sensor, the protons or nuclei of the hydrogen atoms are temporarily subjected to a magnetic field. This aligns the protons to the induced magnetic field and after removing the field, the protons precess about the direction of the Earth's magnetic field. The measured signal generated by the precession gives the intensity of the total magnetic field.

Another type of magnetometer, the fluxgate magnetometer, measures one directional component of the magnetic field, usually the vertical component. It is not as handy in operation as the proton precession meter, and less widely used. It has, however, advantages in areas of very large anomalies, where the direction of the total field varies significantly.

2.5 Interpretation of magnetic field data

Interpretation of magnetic field data generally involves the construction of a model, simulating the distribution of magnetisation in the subsurface material. Such models are commonly assemblages of magnetic bodies, whose location, geometrical shapes and magnetic properties determine their contribution to the anomalous magnetic field. All potential field methods suffer from the fact that an infinite number of models can produce any given response. Successful modelling depends on the ability of the interpreter to impose such initial constrictions to the geometry and magnetic properties, that the ambiguity of the solution is minimal.

Computer methods used for this purpose are in general of two types, the inverse method and the forward method. The former has the advantage of being rapid and is able to give a good fit to the observations with minimal effort of the interpreter. One disadvantage for the inverse method is that it sometimes gives geologically improbable solutions, if the initial constraints are too loose. The latter method involves the computation of the anomaly based on a certain conceptual model given by the interpreter. The advantage of this method is that the interpreter has complete control of the parameters used in the computation. The disadvantage here is that it involves tedious repetitive calculations before a good fit is obtained, and its objectivity can suffer from the preconceptions of the interpreter. Graphical manual methods, can also be

successfully applied, especially for estimating the depth to the magnetic basement, i.e. depth to the top of the individual anomalous bodies.

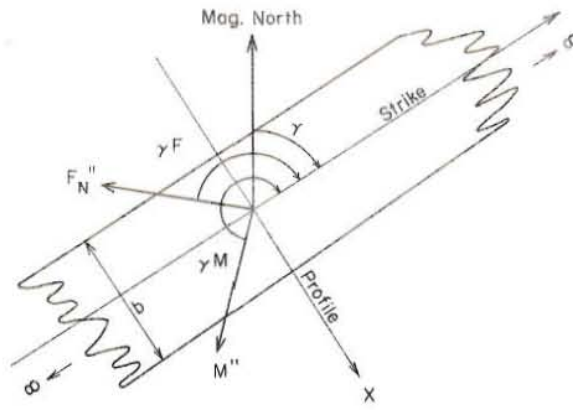
2.5.1 The dyke model

The dyke model has been found to be applicable to a wide range of geological structures. It is a tabular arbitrarily inclined body, infinite in depth and length. The dyke model may be divided into two types, the thin dyke and the thick dyke models. The thick dyke model has a finite thickness, but the thin dyke is assumed to have no thickness, which makes the mathematical expression of its anomaly simpler. In practice a tabular body which has a width b roughly less than the depth of burial d , ($0 < b/d < 1$) can be approximated by the thin dyke model. Wider bodies can be simulated by the thick dyke model.

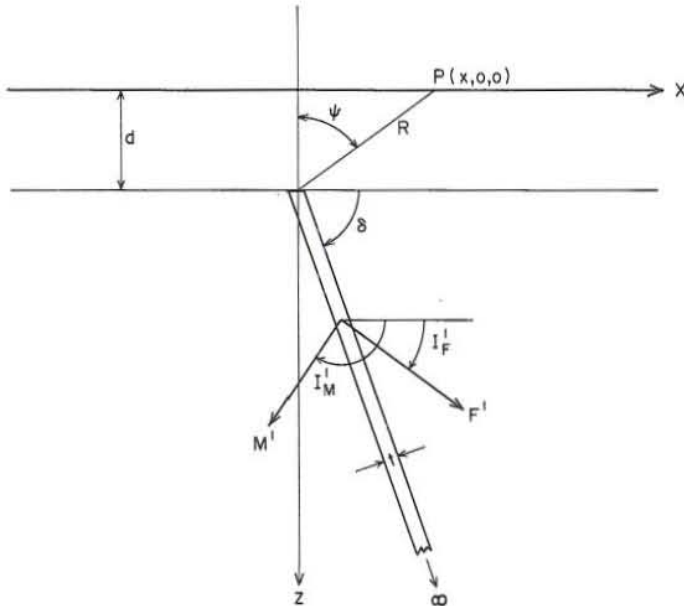
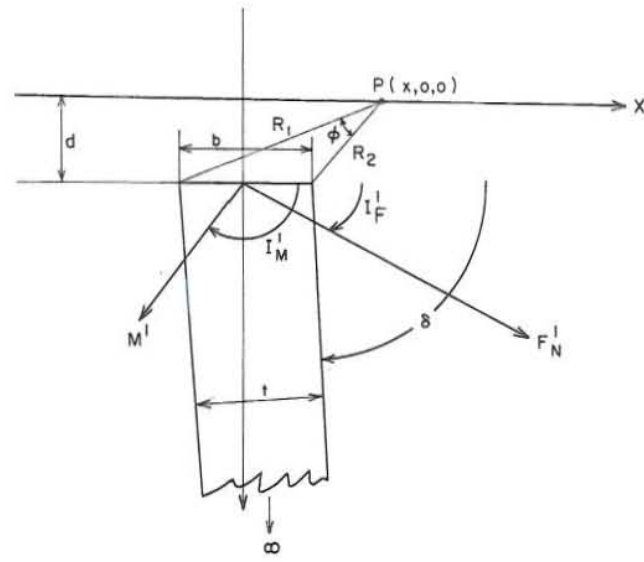
Gay (1963) showed the magnetic anomalies for the infinite dyke model to belong to a single mathematical family of curves for all values of the dip and the strike of the dyke, and all values of the inclination of the magnetizing field. As presented by Am (1972), the general equation for the total field anomaly along a profile normal to the strike of the thin dyke (Fig. 2.4) is of the form

$$\Delta F = -C_F' \cdot \cos\psi \cdot \sin(\psi - \theta) \quad (2.14)$$

where ΔF is the magnetic anomaly (either as ΔZ , ΔH , or ΔF); C_F' is the coefficient term = $2M'(t/d F'/F)$; ψ is the vertical angle ($\arctan x/d$) measured from the top of the thin dyke to the point of observation P in the profile; and $\theta = I_M' + I_F' - \delta$. I_M' and I_F' are the inclination of the effective magnetisation and the normal field vector respectively, projected onto the vertical x - z plane of the profile line; and δ is the dip of the dyke. All these angles are measured from the positive x -axis downwards.



(a) Plan View



(c) Thin dyke, (cross-section)

Fig. 2.4 The dyke model (Am, 1972).

The primed (*) symbol denotes the projection of the components in the xz-plane.

The thick dyke equation can be derived by using the thin dyke equation as an integration element and is given by :

$$\Delta F = C_F (\phi \cdot \sin \theta + \cos \theta \ln(R_2/R_1)) \quad (2.15)$$

where $C_F = 2M' \cdot (F'/F) \cdot \sin \delta$.

If one side of the thick dyke is placed at infinity, the resulting body is a semi-infinite block, resembling a faulted boundary or a geological contact (Fig. 2.5). In this case the amplitude of the anomaly becomes infinite. This model can however be used to simulate the anomaly over a contact, if the far edge of the dyke is placed at a large but finite distance away, thus giving a large but constant contribution to the magnetic field. The semi-infinite block equation then reduces to:

$$\Delta F = C_F (\phi \cdot \sin \theta - \cos \theta \cdot \ln R_1) + C \quad (2.16)$$

where $\phi = \pi/2 + \arctan(x/d)$; and C is an arbitrary constant.

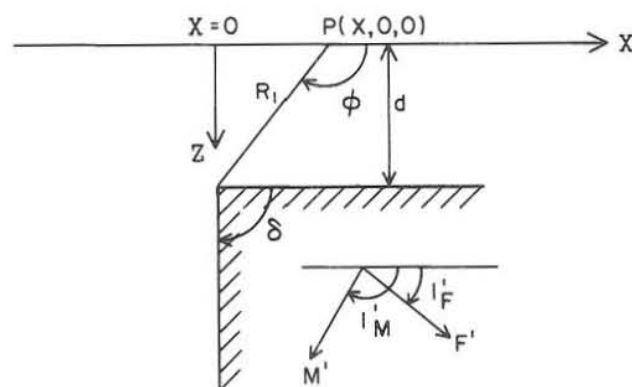


Fig. 2.5 The semi-infinite block model (Am, 1972).

2.5.2 Interpretation by characteristics

This method involves the graphical approach to the solution of magnetic anomalies. Gay (1963) and Am (1972) constructed a complete set of normalized standard curves based on the formulas derived from the dyke models, and these are shown in Fig. 2.6. It follows from the dyke equation that the form of the normalized magnetic anomaly profile normal to the strike of the dyke is dependent only on the parameters b/d and θ . Hence, the solution to the dyke problem involves the determination of the dyke parameters. Determination of these parameters makes use of charts or characteristic curves computed from the dyke equation. Characteristics are dimensionless ratios of two easily definable distances or lengths on a profile. Am (1972) constructed such interpretation charts based on the positions of inflection points, (maximum slope) and half-maximum slope points on the flanks of the anomaly (Fig. 2.7 and 2.8). Good charts of this type give a one-to-one relationship of two characteristic ratios, for all possible values of the b/d and θ parameters. Rao and Babu (1981) also constructed nomograms based on the minimum and maximum points on magnetic profiles due to a long tabular body, in intermediate latitudes. Once the dyke parameters have been obtained, depth can easily be found using depth estimators, obtained from the horizontal positions of the characteristic points. Fig. 2.9 shows interpretation charts (Am, 1972) used in the present work.

A dyke anomaly has in general a principal peak and an associated low. The peak is of larger amplitude, and is defined here to be the positive one, to simplify the discussion. The flanks of the peak are called the steeper flank, which faces the low, and the gentler flank. The gentler flank is the one that is usually more disturbed, and therefore its characteristic points are less reliable.

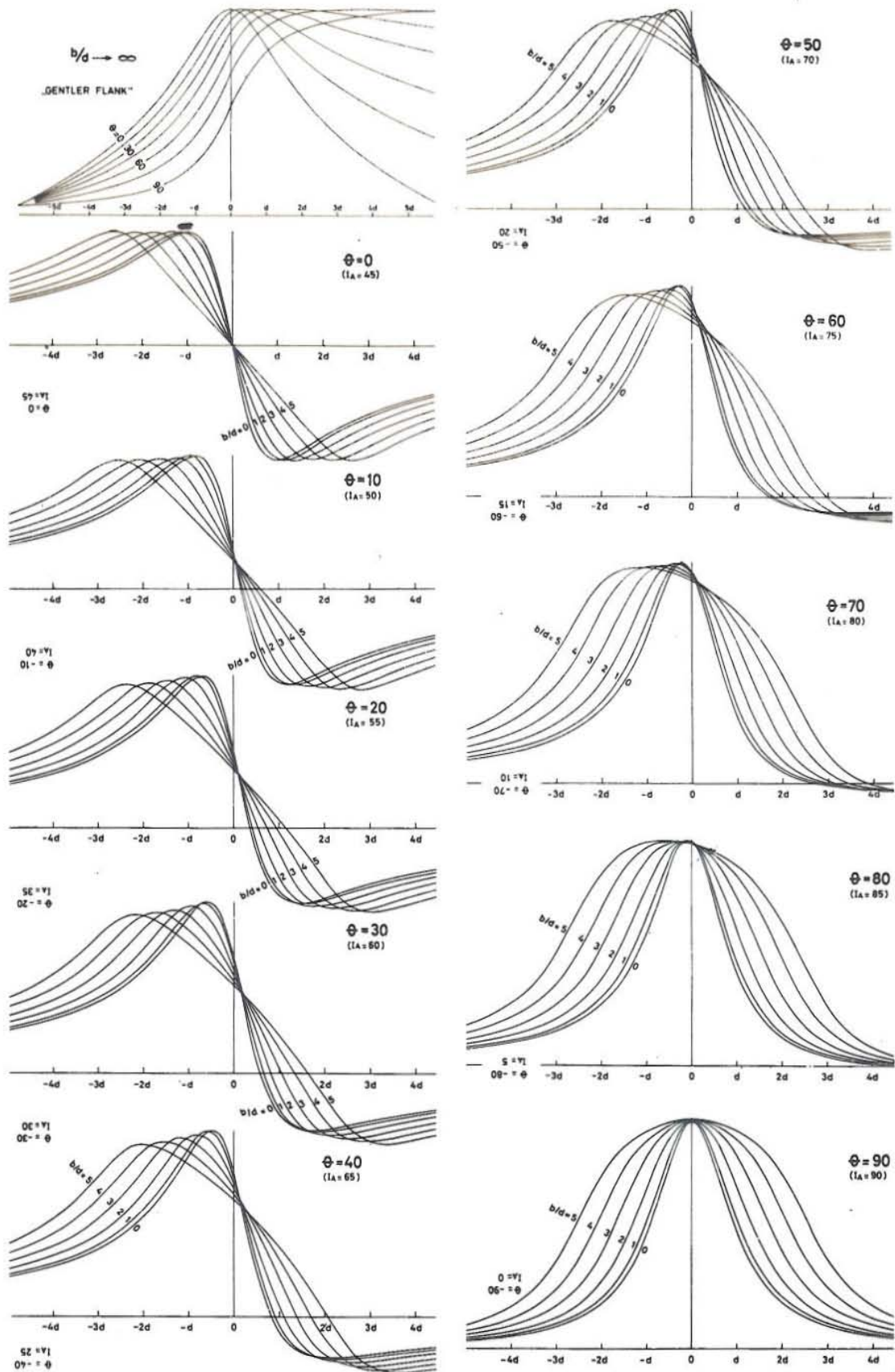


Fig. 2.6 Normalized standard curves for magnetic anomalies due to dykes (Am, 1972).

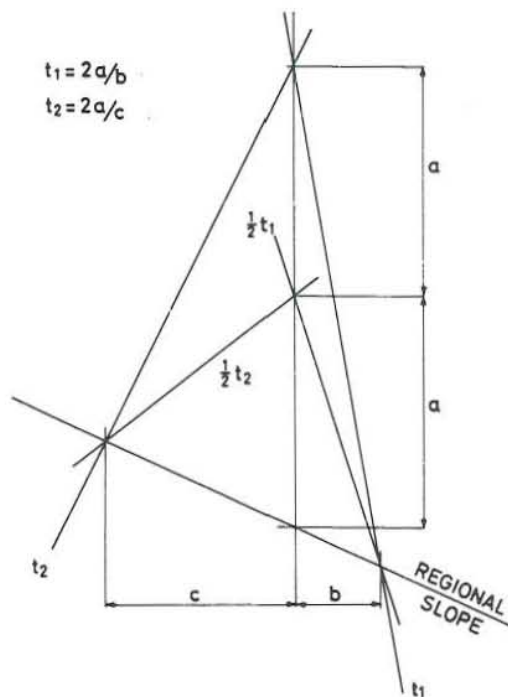


Fig. 2.7 Maximum and half-maximum slopes superimposed on a linear, regional field (Am, 1972).

Some common depth estimators are the so called Peters' length, Sokolov's length and Top length. Their values are dependent on the dyke parameters. The Peters' length (P) (Fig. 2.8) is the horizontal distance between the points of the half-maximum slope and can be obtained from both the steeper flank and the gentler flank. Sokolov's length (S) is the horizontal distance of the inflection tangent on the steeper slope as it rises from minimum to maximum. The Top length (T) is the horizontal distance between the inflection point tangents of both slopes, at the peak level of the anomaly. Depth estimators, obtained from the charts (Fig. 2.10) are given in units of depth to the top of the body. They therefore give a solution for the depth, when compared to the measured value of the depth estimators.

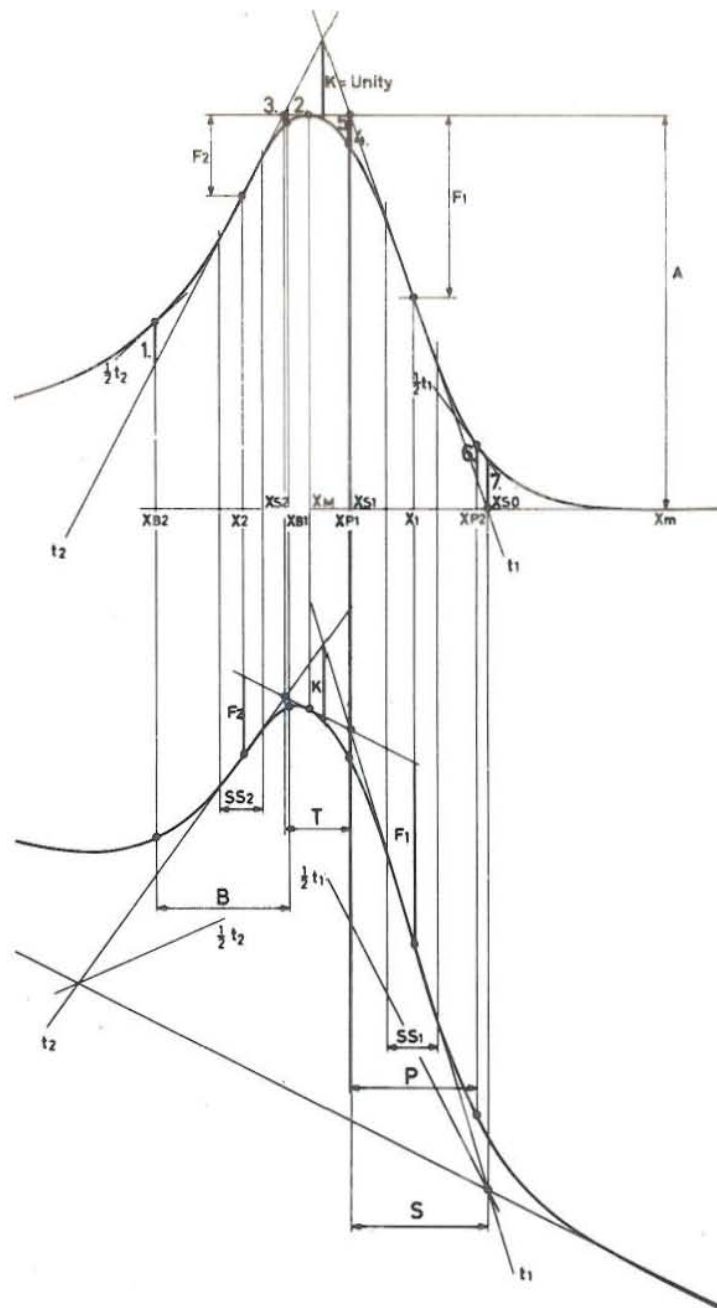


Fig. 2.8 Definition of symbols and lengths used in the interpretation charts. P and B denote Peters length, S denotes Sokolov's length, and T denotes the Top length (Am, 1972).

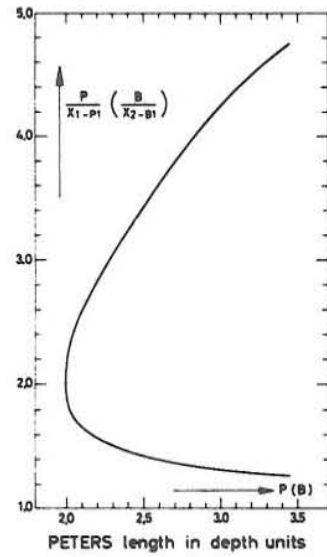
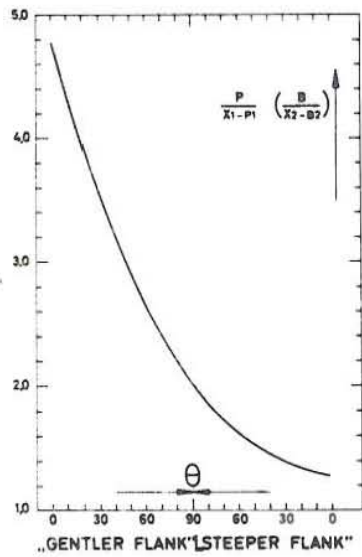
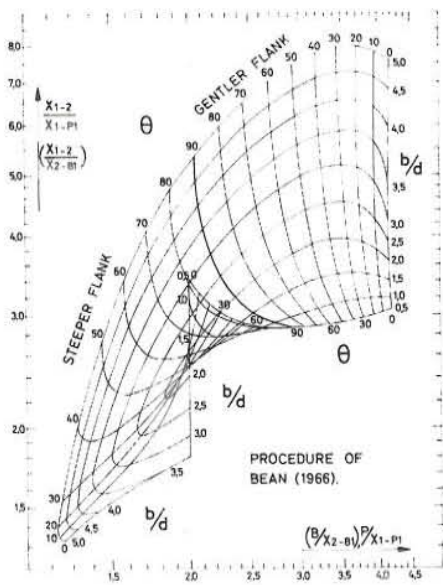
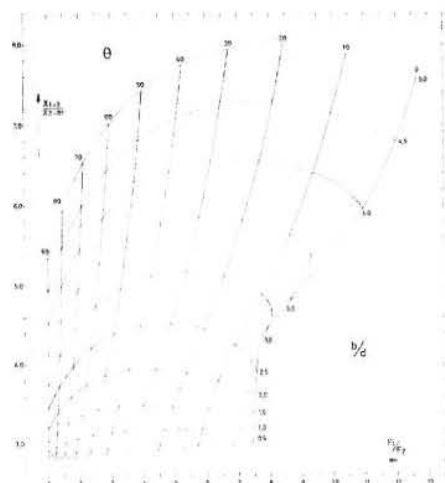
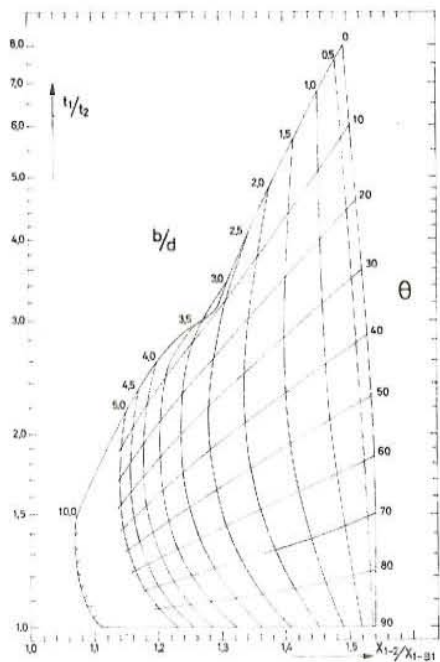


Fig. 2.9 Interpretation charts for determining dyke parameters b/d and θ : (a)-(c) dyke models, (d) semi-infinite block model (Am, 1972).

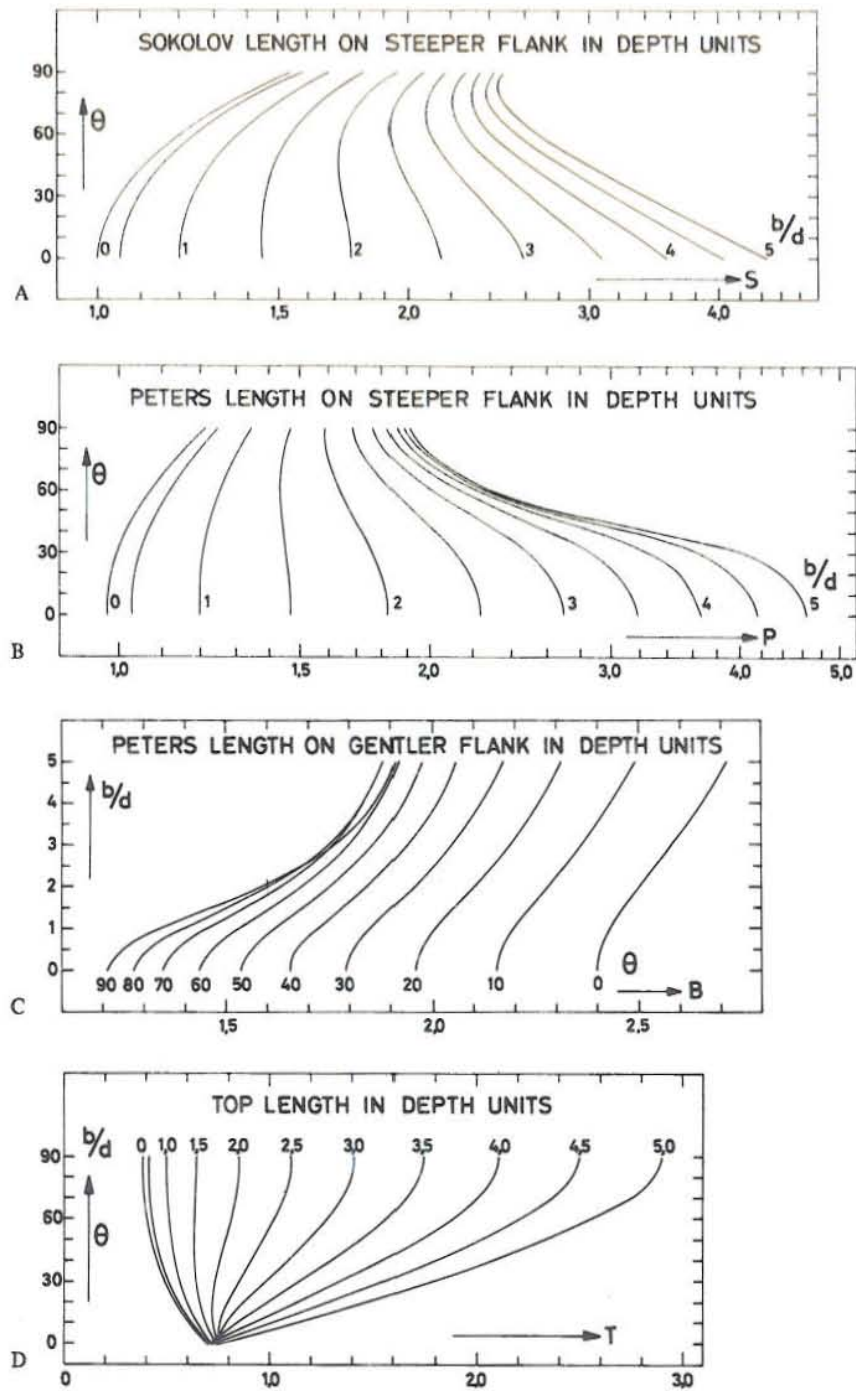


Fig. 2.10 Charts for making depth estimates (Am, 1972).

2.5.3 Computer model interpretation

Due to the inherent ambiguity in the interpretation of potential field data, it is not always advisable to go straightforward into model calculations without having a rough idea about the causative bodies. First of all, the geology of the area is considered, including a study of all available information on the range of values of the intensity and inclination of the magnetisation of the local rocks, and their distribution. From the attitude and shape of the magnetic anomalies it can be inferred whether they can be interpreted by a dyke, semi-infinite block, spherical or cylindrical models, etc.

Two computer programs which are commonly used at NEA in Iceland, have been applied in this work. The program "HALLI" is based on a single thick dyke model, and computes automatically a 'best fit' solution to the dyke anomaly (Fig. 2.11). This is achieved by non-linear method using least squares criteria. The other program "MAG2D" calculates the anomalous field caused by an assemblage of 2-dimensional magnetic bodies defined by a polygonal outline. This type of program is in common use, and a description of the method can be found in the work of Talwani and Heirtzler (1964). The use of this program involves a trial and error procedure to obtain a good fit to the observed anomalies.

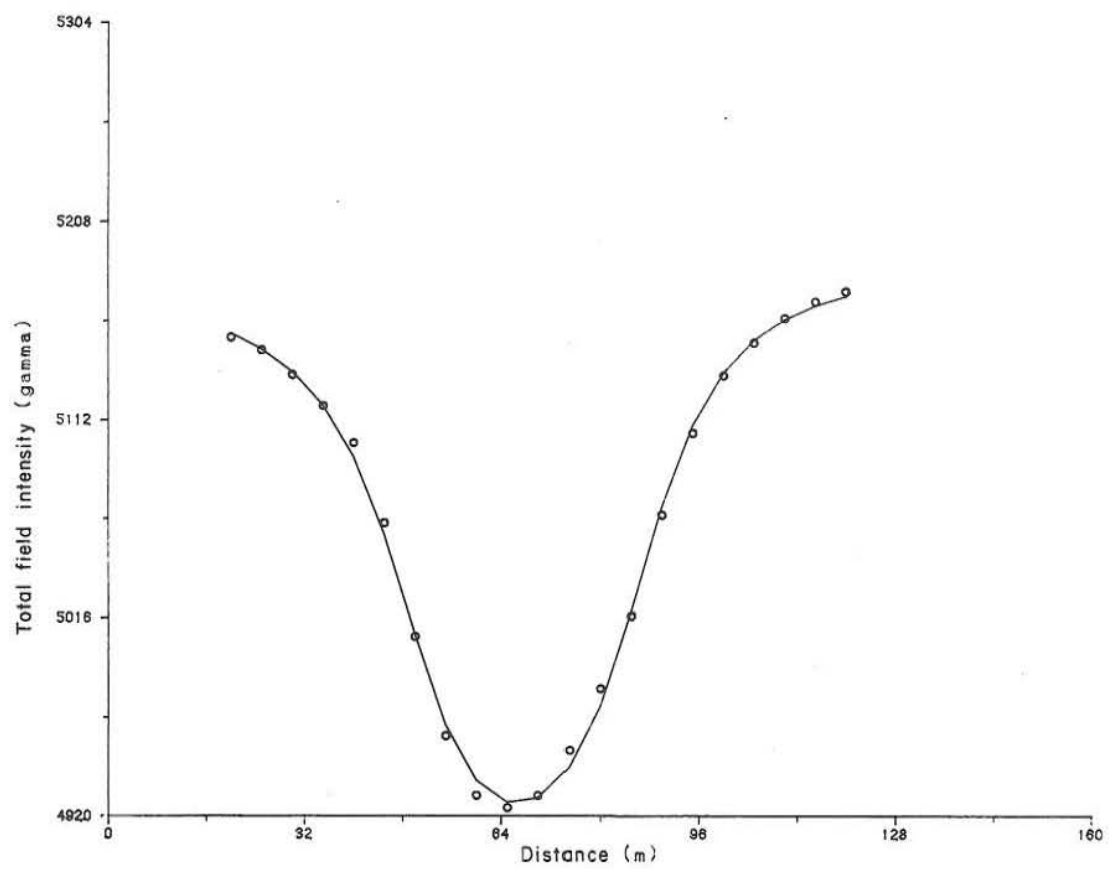


Fig. 2.11 Dyke model computed from the HALLI program. Open circles are measured values and the curve is calculated from the theoretical model.

3 GROUND MAGNETIC SURVEY AT SUMARLIDABÆR, S-ICELAND

3.1 Introduction

Ground magnetic measurements were made near the farm Sumarlidabær, about 10 km NW of Hella, in S-Iceland as part of a training program in geophysical exploration methods (Fig. 3.1). The survey covered an area of 0.12 km², and consisted of 21 profiles spaced 20 m apart and measurements were made at 5 m intervals along each line. Each profile has a total length of 300 m with a bearing of 124 (S 56 E), normal to the regional structure.

In the area of study there are several warm springs or seeps. Since there is little basement exposure near the springs, the purpose of the magnetic survey was to investigate whether some basement structure could be located, which could be interpreted as a conduit for geothermal water to the surface. Such structures are commonly found to be dykes or faults.

The interpretation of the magnetic anomalies encountered is presented here as an application to the magnetic method discussed earlier. The result of this study is not very conclusive, but it does give a rough idea about the structural features involved.

3.2 Geology of the study area

The region under study is in tilted Plio-Pleistocene strata (Hreppar series) east of the Reykjanes-Langjökull active zone of rifting and volcanism, which extends to the SW along the Reykjanes peninsula, where it connects with the spreading axis of the Mid-Atlantic Ridge. Basement outcrops are few in the area. It was noted that in the vicinity of Sumarlidabaer area, the Hreppar series are mainly composed of lava flows with thin, red

intercalations, but with little or no interbeddings of tillites and hyaloclastites. The oldest rocks of the Hreppar series are from the Gauss magnetic epoch, but most of the series are from the Matuyama epoch, and the volcanic strata is thus characterised by alternating layers with normal and reversed magnetic polarity directions (Fridleifsson et al., 1980).

Unconformably overlying the Hreppar series are flat lying interglacial and postglacial lava flows (Saemundson, 1970). These are known to be normally magnetized and dated to be of the Brunhes normal polarity epoch (0-0.7 m.y. old). In the south, the young lavas form an almost continuous sheet with a thickness varying from 5 - 100 m. A thin sedimentary layer is also found to occur below the interglacial lava flows. The measured thickness of this sandstone bed ranges from 1 - 5 m and it is generally thinner in the western part of the area. A few kilometers away from the survey site the underlying Hreppar series are reported to dip 4 - 8° towards NW (Saemundsson, 1970). The dip of the lava units is related to the Hreppar anticline, whose axis is to the east of the Sumarlidabaer area.

The Hreppar series have been much affected by dyke intrusions and faulting. The dykes, which usually occur in swarms in Iceland, are found to be perpendicular to the planes of the lava flows. The measured thicknesses of the dykes vary from 1m to 10 m in outcrops, and they generally trend NE-SW. The normal faults generally trend N 15-30°E and some are reported to have a downthrow of several tens of meters. In the region near Sumarlidabaer three directions of faulting are seen : N 0-10°E, N 60°E, N 20-40°E. The first two are thought to be active faults associated with large recent earthquakes in the area, while the last is considered to be older and probably inactive. Most of the faults are arranged in a step-fault pattern with the downthrow side on the east towards the axis of the Hreppar anticline. The active faults dissect the young lavas.

Several low temperature areas are found in the region, e.g. the Harlaugstadir, Sumarlidabaer and Laugaland areas (Fig. 3.1). Experience in the low temperature areas in Iceland shows that aquifers are commonly connected with fractures, faults and dykes cutting the lava formations (Fridleifsson, 1979). The three geothermal areas mentioned above are arranged on a N 70°E trending line. Warm springs within each area are also found to be linearly arranged, showing a similar trend.

Laugaland is the best studied of these thermal areas (Georgsson et al., 1978; Flovenz and Georgsson, 1982). There the geothermal water is conducted horizontally from NE along a N 40 E trending dyke. The hot water comes to the surface along a N 70°E trending fault or fracture, which cuts the N 40 E dyke. In Laugaland, which is at the bottom of a shallow valley carved through the young interglacial basalts down into the Hreppar series, the basement is covered by 10-20 m of sand and gravel. At our survey site at Sumarlidabaer, the Hreppar series are also thought to form the basement, under a thin cover of superficial deposits. It is also likely that intersecting faults and dykes control the flow of geothermal water, similar to the Laugaland area.

3.3 Magnetic measurements and data processing

A 300 m baseline was initially established by erecting wooden surveying poles along the line. Magnetic measurements were then taken along this baseline at intervals of every 5 m, using a proton precession magnetometer. The total magnetic field intensity, F was recorded in a dictaphone throughout the whole survey. The next succeeding profiles were laid parallel to the baseline at intervals of 20 m. Irregularities in the topography such as canals, etc. were noted while making the measurements. Hot springs near the profile line were also located accurately and their temperatures measured. During

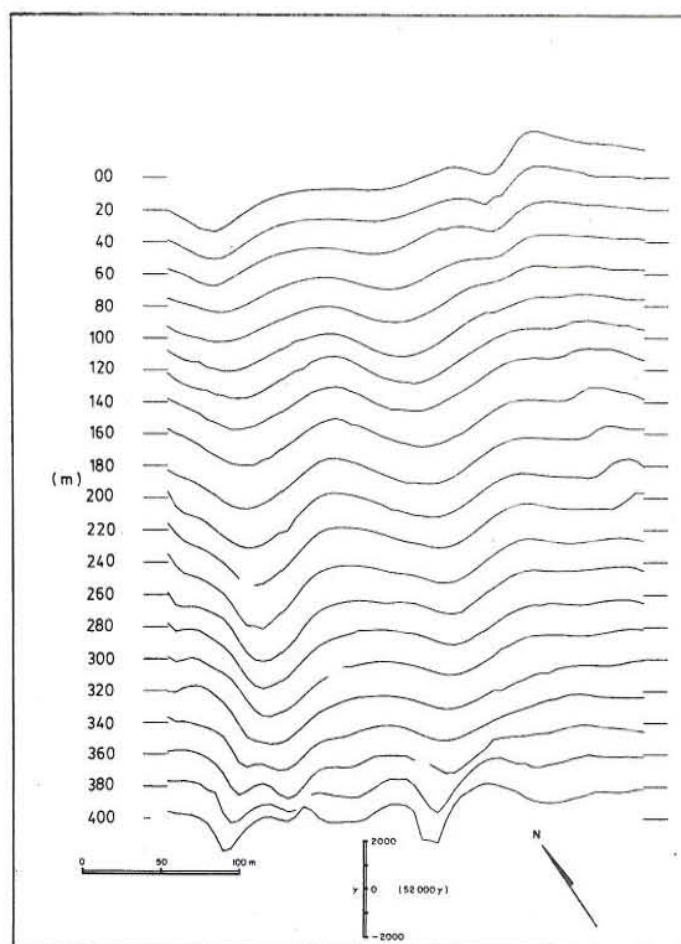
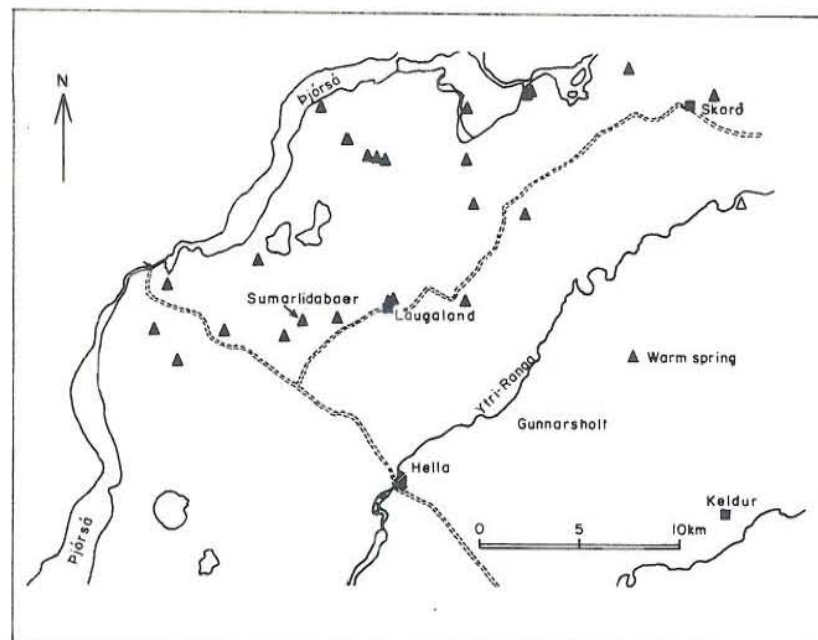


Fig. 3.1 Ground magnetic survey at Sumarlidabaer
 (a) location map, (b) measurement plot.

the field survey, a few repeat readings were taken to insure the accuracy of the measurements. No base magnetometer readings were made because it is unnecessary in regions of high magnetic anomalies.

After the field survey, the measurements were plotted on a sheet of paper and compiled in a datafile in the computer. The data are then plotted as a profile plot (Fig. 3.1). A few suspect readings detected in the profiles were deleted or adjusted graphically to the overall trend of the anomalies. No normal corrections for the spatial variations of the Earth's magnetic field (the IGRF-field) were made, as they are insignificant in this case.

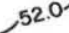



The anomalies of interest, reflecting basement structure, are dominant in the anomalous field, so that no processing, such as band-pass filtering or upward or downward continuation is thought necessary.

In our area the inclination of the magnetic field is 75° and the declination N 20° W.

3.4 Interpretation of the magnetic anomalies

The magnetic anomalies manifested in the total magnetic field intensity map (Fig. 3.2) and in the series of profiles (Fig. 3.1) show the dominant linear trend of the magnetized bodies, about N $30-40^\circ$ E. There are two major anomalies in the survey area, an elongated, narrow negative magnetic anomaly on the lefthand side (west) and a broad positive anomaly on the righthand side (east). The linearity of the negative anomaly is highly indicative of a reversely magnetised dyke body. The flanks of the negative anomaly are almost symmetrical, implying that the dip of the dyke body is near vertical. The broad positive anomaly on the right (east) suggests a fault structure. In the middle part of the area, between the two anomalies previously described, there is a small magnetic low

TOTAL MAGNETIC FIELD
INTENSITY MAP

-  52.0 52.0 x 10³ γ
 -  Ditch
 -  Warm spring temp
 -  Measurement profile
- 0 50m

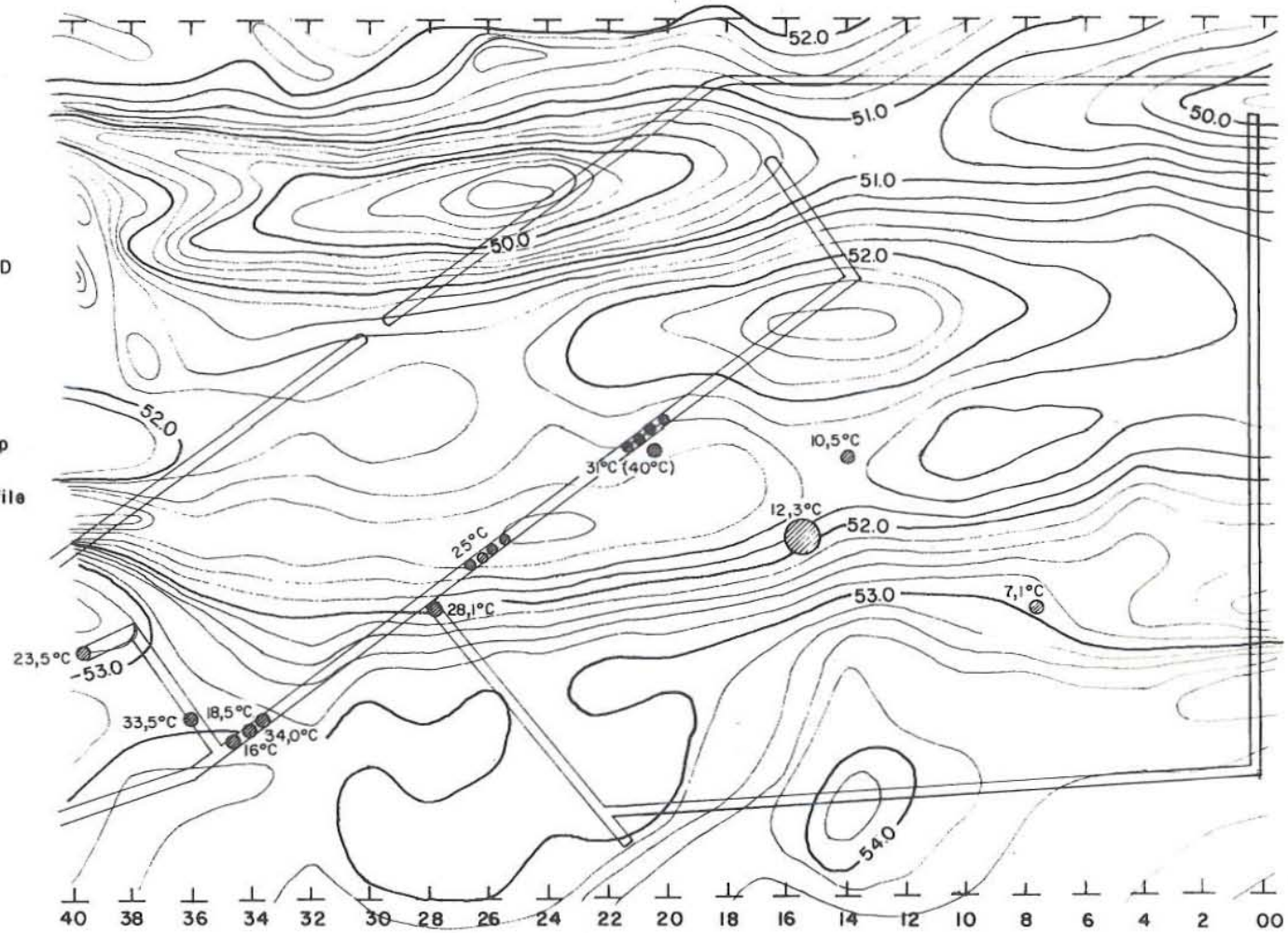
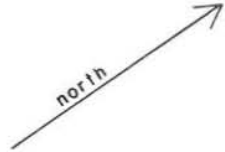


Fig. 3.2 Total magnetic intensity map.

anomaly. This could also be interpreted to be due to a small reversely magnetised dyke body. In the northeast corner of the area, a fault-like anomaly is indicated, trending approximately N-S. In general, the anomalies in the south (profile line-40) are sharper and contain higher frequencies than the anomalies in the north (profile line-00), which means that the depth to the magnetic basement is less in the southern part.

3.4.1 Assumptions and guidelines to interpretation

Quantitative interpretation of potential field anomalies require the use of several assumptions, since most of the parameters used in the calculations are virtually unknown. In this study, some of these are:

(1) The magnetisation for each of the magnetised bodies was allowed to take an independent value in the solutions obtained from the various profiles. Since no measurements were made on the magnetic susceptibilities of the rocks in Sumarlidabaer, the intensity of magnetisation was inferred to be of the value obtained from the best fit solution of the "HALLI" program.

(2) The remanent magnetisation of the basement geological formations was assumed to be dominant over the induced magnetisation. The direction of magnetisation, or the magnetisation contrast, could therefore vary from one place to another. This view is supported by the observations of Kristjansson (1977) on Icelandic rocks, which indicate that Q is generally greater than 1 and that the direction of the remanence is highly variable. Q is the Koenigsberger ratio, which is the ratio between the remanent (R) and the induced magnetisation (M).

(3) The dyke intrusives in the model have a higher intensity of magnetisation than the basaltic lava flows.

(4) The regional anomaly is assumed to be constant throughout each profile. This is an important assumption since identification of anomalies depends very much on the regional background.

3.4.2 Methods of interpretation

The graphical and numerical methods discussed earlier, were used in the interpretation process. Emphasis was put on trying out these methods on the prominent reversely magnetised dyke. The dyke parameters were initially obtained by the graphical method. Depth estimates were made using the Peters' length on the steeper flank, but in some cases the gentler flank was used. A combination of the sets of nomograms, given by Am (1972), were used to find a good estimate of the dyke parameters. The results from the graphical method are tabulated in Table 1.

Numerical calculation was then carried out using as initial estimates the parameters obtained from the graphical method. A segment of the profile was then selected and interpreted, using a single infinite dyke model. All calculations were done by the computer using the "HALLI" program. The computer optimizes the model automatically by adjusting the parameters until it finds a good fit for the anomaly. Each of the parameters can be fixed if their likely values are known. The calculated models are listed in Table 1. Fig. 3.4 shows the depth to the top of the dyke in a section along its length.

Entire observation lines are then interpreted quantitatively using 2-dimensional arbitrarily magnetised bodies (MAG2D program). Each body has a homogeneous magnetisation. The computed models are shown in Figs. 3.5-3.7.

Table 1. Estimated parameters for the reversely magnetised dyke

Line	Graphical			Numerical				
	θ	b/d	d (m)	x (m)	b (m)	d (m)	Msin δ	$I_M - \delta$
00	-	-	-	30.4	20.5	24.9	-1.23	-23.25
02	74	1.5	22	33.5	25.9	24.6	-0.93	-29.52
04	75	2	23	32.8	13.7	27.8	-1.78	-29.71
06	59	0.6	37	42.2	24.2	32.4	-1.14	-40.10
08	80	1.2	33	38.5	47.5	47.5	32.4	-27.51
10	82	2.2	30	45.5	37.2	31.5	-0.87	-33.25
12	-	-	-	58.2	37.8	32.0	-0.98	-37.24
14	61	4	19	50.0	46.9	26.5	-0.75	-25.27
16	85	1.9	27	53.3	46.0	27.3	-0.89	-25.00
18	75	4.5	20	57.1	46.3	21.3	-0.72	-32.86
20	81	1.75	24	67.2	46.7	14.1	-0.55	-41.72
22	-	-	-	67.8	40.5	13.7	-0.62	-35.05
24	81	3.5	18	61.4	37.6	12.6	-0.67	-23.51
26	-	-	-	63.1	37.0	11.6	-0.65	-16.69
28	80	3.4	12	62.9	30.0	20.8	-1.25	2.70
30	69	3.9	11	67.9	32.2	19.4	-1.01	-2.29
32	80	2.1	13.6	62.4	40.1	16.5	-0.78	-11.24
34a	-	-	-	47.2	6.93	9.9	-1.09	56.98
34b	-	-	-	84.6	16.0	18.4	-1.02	-54.54
36a	-	-	-	43.9	11.1	11.2	-1.04	3.30
36b	-	-	-	84.5	17.2	8.0	-0.39	-40.58
38a	-	-	-	38.9	11.0	9.0	-0.94	50.4
38b	-	-	-	88.2	15.7	5.6	-0.22	-70.27
40	-	-	-	41.6	6.2	8.51	-1.26	-3.74

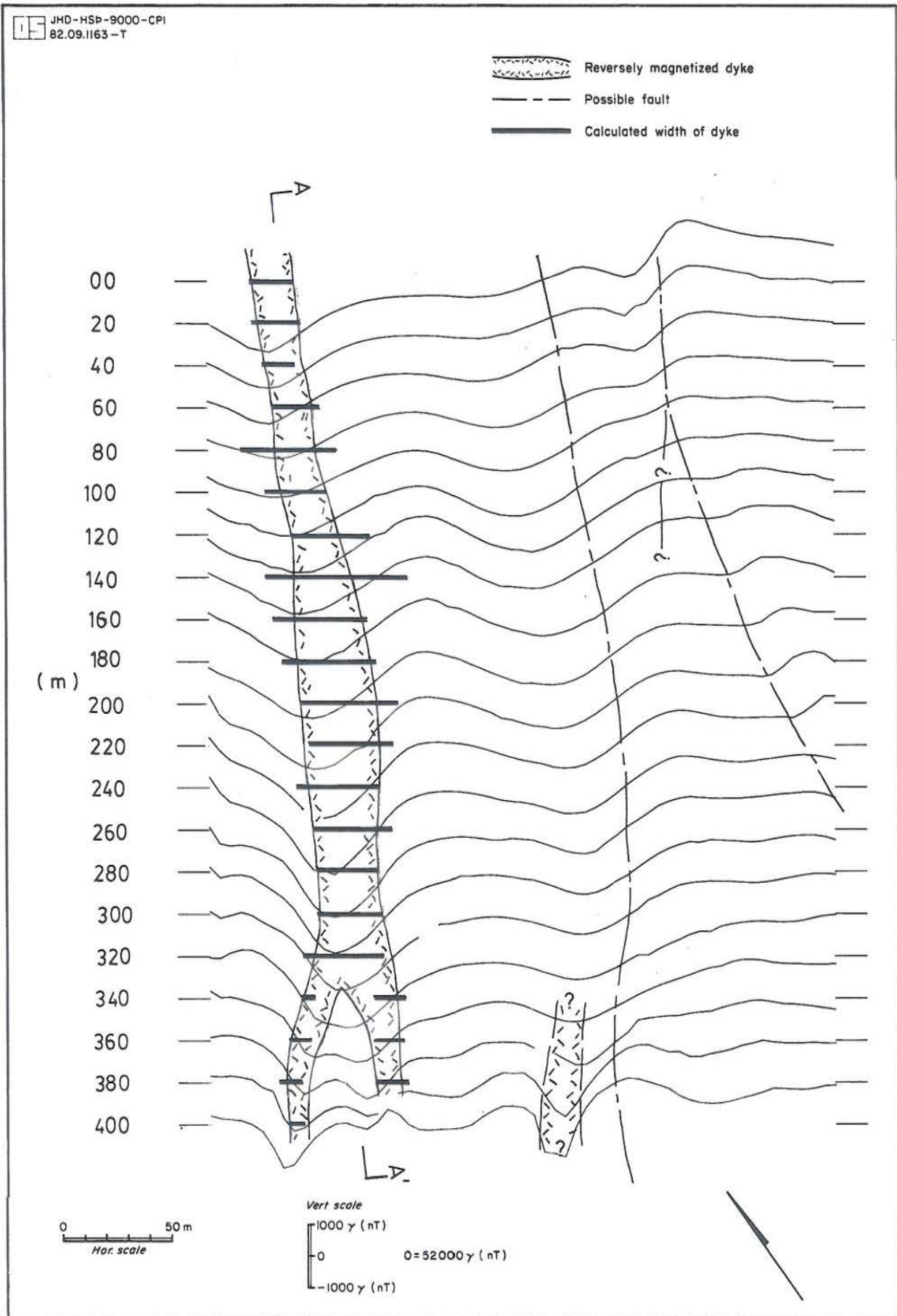


Fig. 3.3 Interpreted dyke and fault model.

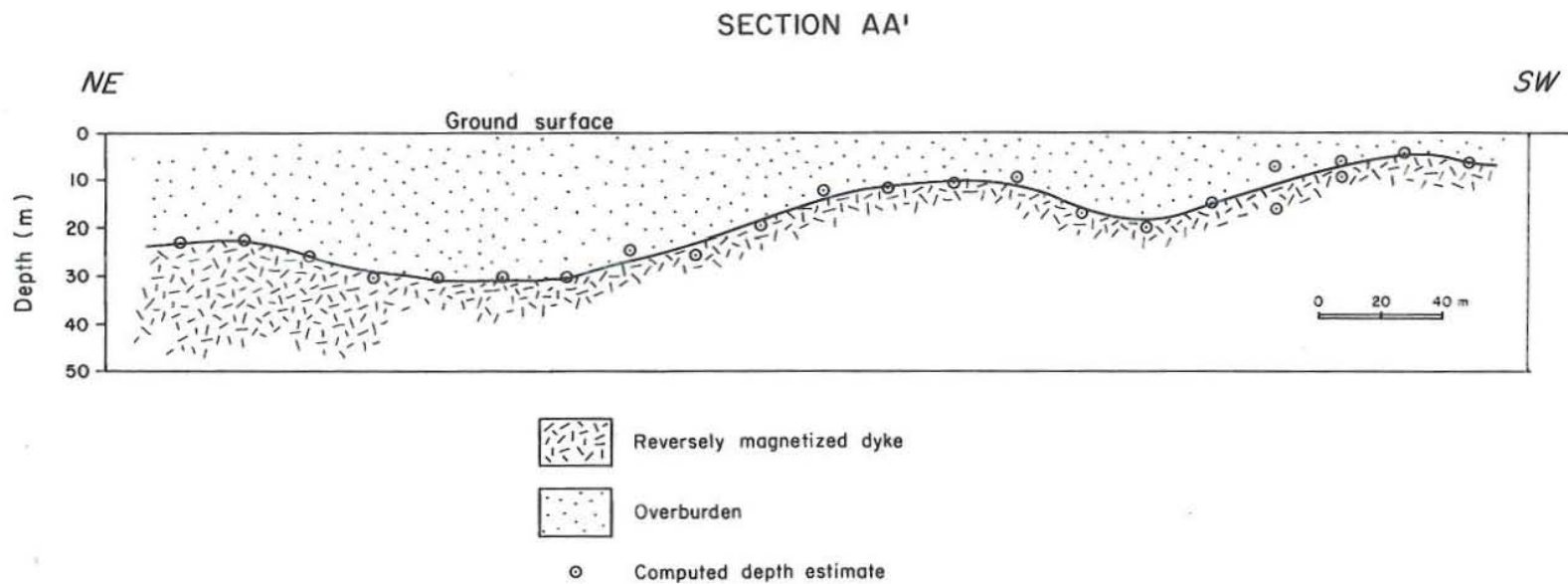


Fig. 3.4 Top of the reversely magnetised dyke body.

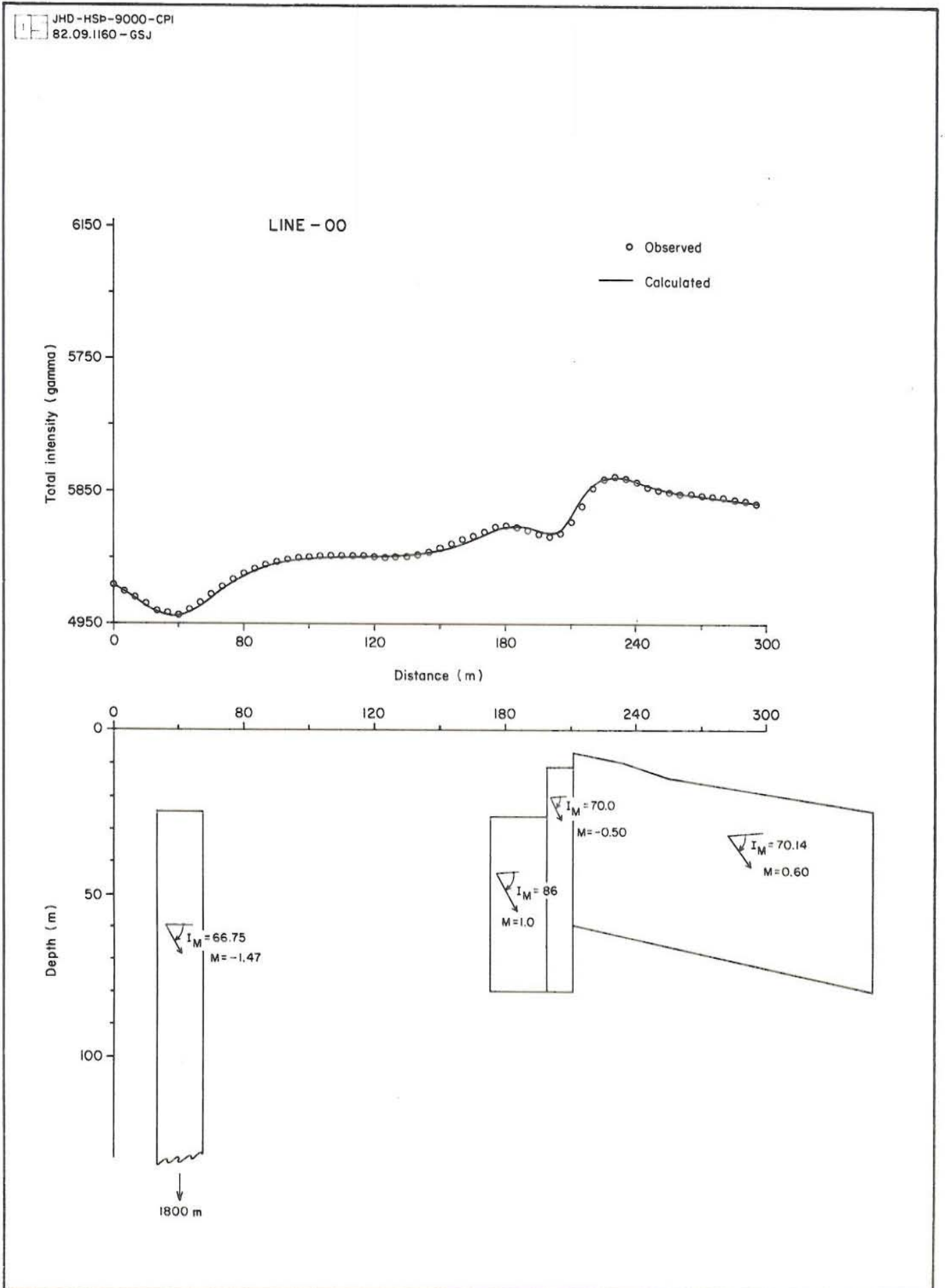


Fig. 3.5 Interpreted 2-dimensional model along line-00.

JHD-HSP-9000-CPI
82.09.1161-GSJ

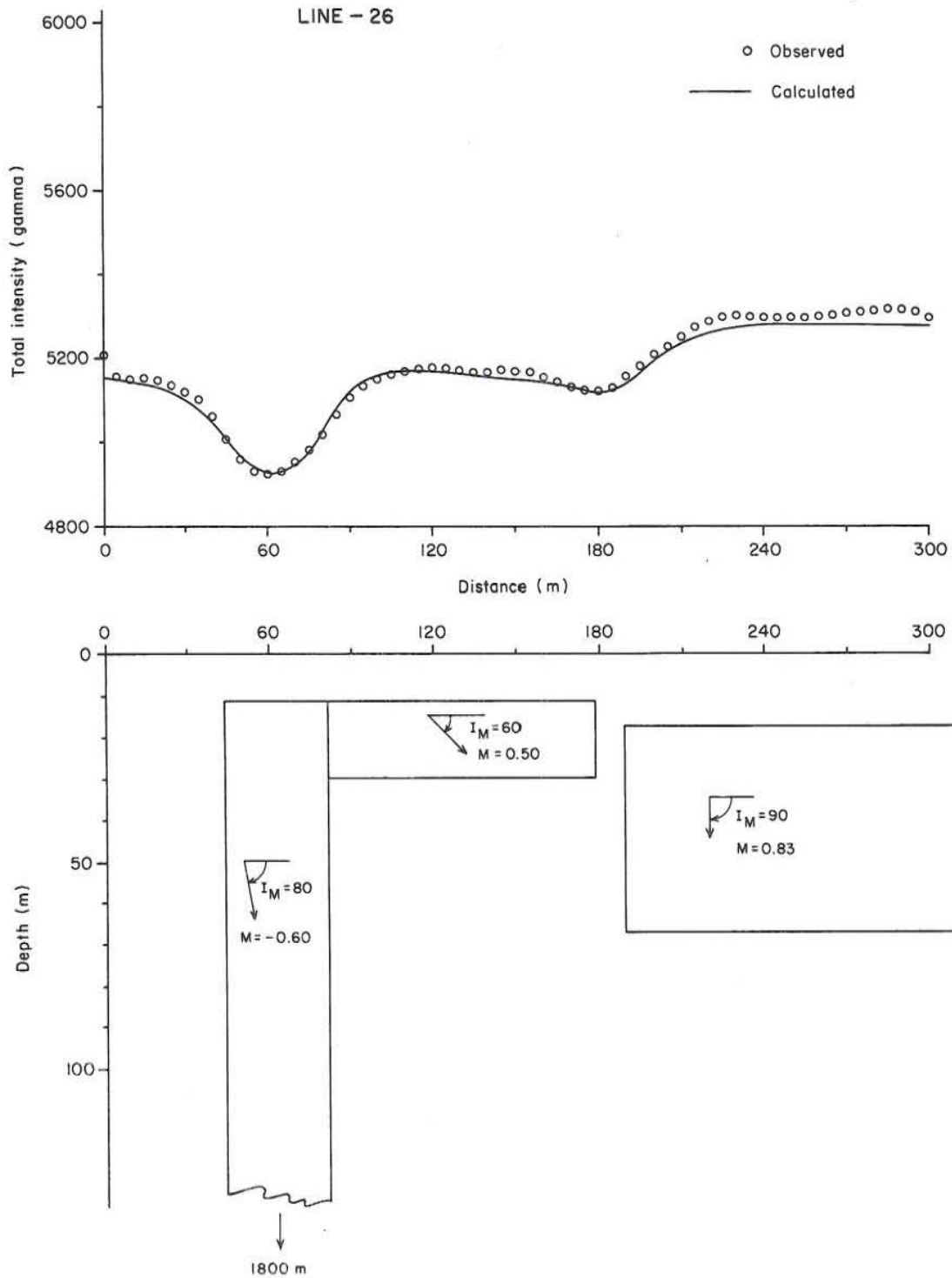


Fig. 3.6 Interpreted 2-dimensional model along line-260.

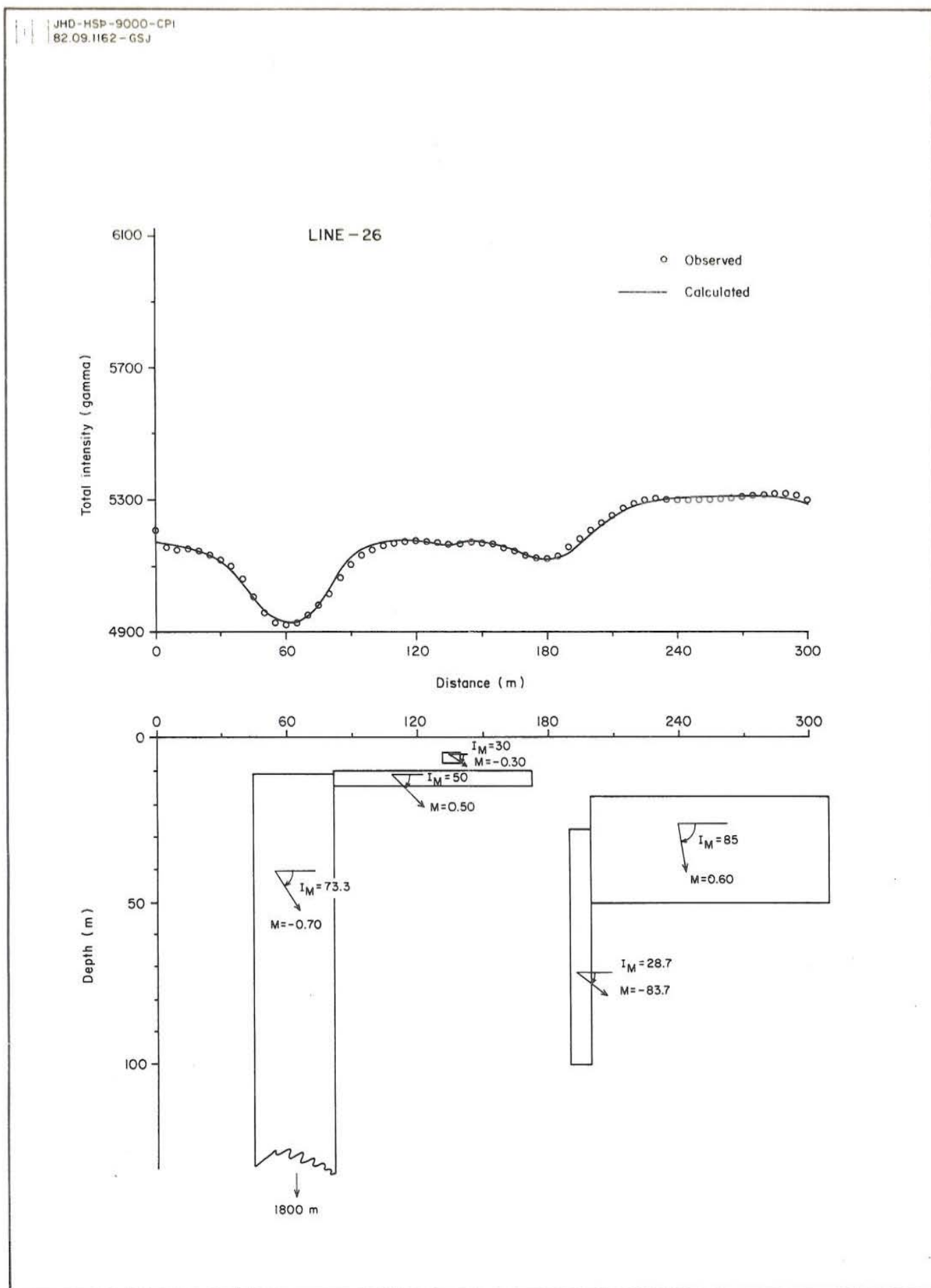


Fig. 3.7 Interpreted 2-dimensional model along line-260 using different parameters.

3.4.3 Summary of the results

Based on the results obtained from the graphical and numerical methods, the magnetic anomalies in the area surveyed are caused by a reversely magnetised dyke on the western side and possibly a fault structure on the eastern side of the map. The depth to the basement, as indicated by the dyke solutions, is about 25 m in the line-00, deepens somewhat towards the south and then goes up to about 8 m in line-40. Generally, the basement is estimated to slope gently towards the north. The strike of the dyke is about N 30°E, in line with the general trend in the region. The average width of the top of the dyke is approximately 30 m. The θ parameter of the dyke body was calculated to be near vertical (60-85). The dip of the dyke cannot be uniquely determined, because the inclination of the effective magnetisation, largely caused by the remanence, is virtually unknown.

The other magnetic anomaly, to the east in Fig. 3.3, looks as though it is caused by a fault structure. The graphical method using characteristics for a contact or "fault" model gave an average depth to basement estimate of about 10-20 m. Another linear feature, probably a N-S trending fault is indicated at the bottom left corner of the map.

Two-dimensional model calculations based on a dyke and a fault model for the magnetic anomalies are given in Figs. 3.5 to 3.7. These modelling attempts indicate that the eastern anomaly could be caused by a fault and a small adjacent magnetised dyke. However, it is also possible that there is only a fault present, or possibly multiple faults possessing a complex magnetisation contrast. It can be said here that the fault and dyke model for the magnetised anomalies is possible. Several other models were tried, but the results are not feasible.

3.5 Conclusions

The dip of the dyke cannot be determined because the magnetisation vector M is unknown. However, it can be inferred based on the geological evidence made by previous workers. It is known that dykes in the area usually intrude perpendicularly to the lava formations. If this 'rule of thumb' applies in S-Iceland, then the reversely magnetised dyke is possibly dipping a few degrees SE, since the Hreppar series dip to the NW. A fault was interpreted by magnetic evidence to be nearby, about 135 m to the NE away from the dyke. If the fault exists and is assumed to be vertical with a downthrow on the eastern side (see model on Fig. 3.5-3.7), then it is likely to intersect the dyke at a certain depth. Other workers (Saemundsson, 1970) have noted that the dip of the lavas of the Hreppar series nearby Sumarlidabaer is about $4-8^\circ$. Using 8° as the maximum dip of the lavas then it can be easily calculated that the minimum depth at which the fault would intersect the dyke is at 960 m.

It is interesting to note that several warm springs occur along the place where the magnetic anomalies are interpreted to be due to a fault structure (Fig. 3.2). Near the surface, the interpreted dyke and the fault are almost parallel such that they do not intersect in the area of the hot springs. However, if they cross at depth it could be inferred that the hot water flows upwards along the dyke and then percolates through the fault.

The trend of the major features, the dyke and the fault-dyke complex, is $N 30^\circ E$, which is similar to the strike of the dyke at the Laugaland hydrothermal area (Fig. 3.1). These structures could in a similar way conduct thermal water to the area from the NE. The indication of N-S trending fault, which is reported as being recently active, could be of importance. These faults might have small displacements, and therefore not easily discovered by magnetic surveying. Their importance

as potential water channels is however as great, and they could act as conduits for hot water to the surface.

Other geophysical methods such as VLF (very low Frequency) or the "head-on" resistivity profiling methods could be tried to verify the existence of the vertical structures.

In spite of the elaborate methods of interpretation used for the magnetic anomalies, the results are still ambiguous. Even if the shape of the main anomalous bodies has been assumed to be dyke or fault-like, a whole range of models giving an acceptable fit to the observed anomalies is still possible. Difficulties in the interpretation are partly caused by the lack of resolution, i.e. the distortion of closely spaced overlapping anomalies. An even greater source of ambiguity is the arbitrary direction of magnetisation, or more correctly magnetisation contrast, which can be expected in Icelandic basalt formations. This fact stresses the feasibility of a more systematic investigation of the magnetic properties of the rocks in the survey area.

ACKNOWLEDGEMENTS

I wish to thank the organizers of the 1982 UNU Geothermal Training Programme, the Icelandic government and The United Nations University for granting me this fellowship. I am deeply indebted to Mr. Karl Gunnarsson for his guidance, close supervision and useful advises during the course of my study in magnetics; to Dr. Axel Bjornsson, Messrs. Ludvik S. Georgsson, Gylfi Pall Hersir, Olafur Flovenz and Halldor Halldorsson for providing me the wealth of information on the resistivity method; and to Dr. Valgardur Stefansson, Messrs. Steinar Gunnlaugsson, Benedikt Steingrimsson and Gudjon Gudmundsson for their assistance during my brief training in borehole geophysics. My special thanks are due to Dr. Ingvar Birgir Fridleifsson for his lectures and for critically reviewing the manuscript; to Mr. Sigurjon Asbjornsson for typing some of the manuscript; and to Ms. Sylvia Johannsdottir for drafting most of the figures. My sincere gratitude is also due to the management of PNOC-EDC Geothermal Division, in particular to Mr. Bernardo S. Tolentino for their support in making this study possible.

REFERENCES

- Am, K., 1972. The arbitrary magnetized dyke: interpretation by characteristics. *Geoexploration*, 5: 63-90.
- Baranov, V., 1975. Potential fields and their transformations to applied geophysics. *Geoexploration Monographs, Series 1-No. 6*, Geopublication Associates, Berlin, 119pp.
- Baranov, V. and Naudy, H., 1964. Numerical calculation to the formula of reduction to the magnetic pole. *Geophysics*, 29(1): 67-79.
- Bhattacharyya, B. K., 1965. Two dimensional harmonic analysis as a tool for magnetic interpretation. *Geophysics*, 30(5): 829-857.
- Bhattacharyya, B. K., 1967. Some general properties of potential fields in space and frequency domain: A review. *Geoexploration*, 5: 127-143.
- Bhattacharyya, B. K. and Leu, L., 1975. Analysis of magnetic anomalies over Yellowstone National Park: Mapping of the Curie point isothermal surface for geothermal reconnaissance. *Journal of Geophysical Research*, 80(32): 4461-4465.
- Bjornsson, A., 1981. Exploration and exploitation of low temperature fields for district heating in Akureyri, N-Iceland. *G.R.C. Transactions*, 5: 495-498.
- Breiner, S., 1973. Applications manual for portable magnetometer, Geometrics, California, 58pp.
- Flovenz, O. G. and Georgsson, L. S., 1982. Prospecting for near surface vertical aquifers in low temperature geothermal areas in Iceland. Paper submitted to the Geothermal Resources Council Transactions 6.

- Fridleifsson, I. B., 1979. Geothermal activity in Iceland. *Jokull*, 29: 47-56.
- Fridleifsson, I. B., Haraldsson, G. I., Georgsson, L. S., Gunnlaugsson, E. and Bjornsson, B. J., 1980. Regional geothermal exploration in Gnupverjahreppur district. Orkustofnun report OS80010/JHD06, 136pp., (in Icelandic).
- Gay, S. P., 1963. Standard curves for interpretation of magnetic anomalies over long tabular bodies. *Geophysics*, 28: 161-200.
- Georgsson, L. S., Johannesson, H., Kjartansdottir, M. and Gunnlaugsson, E., 1978. Laugaland i holtun, jarðhitakönnun og borun holu 3. Orkustofnun, OS JHD 7802.
- Grant, F. S. and Martin, L., 1966. Interpretation of aeromagnetic anomalies by the use of characteristic curves. *Geophysics*, 31: 135-148.
- Grant, F. S. and West, G. F. 1965. Interpretation theory in applied geophysics. McGraw-Hill Book Company, New York, 584pp.
- Gupta, V. K. and Fitzpatrick, M. M., 1971. Evaluation of terrain effects in ground magnetic surveys. *Geophysics*, 5: 582-589.
- Henderson, R. G. and Zeitz, I., 1967. The computation of second vertical derivatives of geomagnetic fields. *Mining Geophysics, Society of Exploration Geophysicists*, 1: 606-614.
- Hunt, T. M. and Smith, E. G. C., 1981. Magnetisation of some New Zealand igneous rocks. *Journal of the Royal Society of New Zealand*, 12(2): 159-180.

- Kristjansson, L., 1977. Some measurements and computations relevant to the magnetic layer thickness estimates in Iceland. Science Institute report, RH-77-1, 21pp.
- Nagata, T., 1961. Rock Magnetism. Maruzen Company Ltd., Tokyo, 350pp., Revised edition.
- Palmasson, G., 1975. Geophysical methods in geothermal exploration. Proceedings of the Second UN Symposium on the development and use of geothermal resources, San Francisco, 2: 161-200.
- Parasnis, D. S. 1973. Mining Geophysics. Elsevier Scientific Publishing Co., Amsterdam, 395pp.
- Paul, P. A. and Roy, A., 1967. Magnetic interpretation on uneven topography. *Geoexploration*, 5: 205-225.
- Pedersen, L. B., 1979. Wavenumber domain methods for fast interpretation of potential field data. *Geoexploration*, 17: 205-221.
- Peters, L. J., 1949. The direct approach to magnetic interpretation and its application. *Geophysics*, 14: 290-320.
- Rao, D. A. and Babu, H. V. R., 1982. Nomograms for the rapid evaluation magnetic anomalies over long tabular bodies. *PAGEOP*, 119: 1037-1050.
- Reford, M. S., and Sumner, J., 1964. Aeromagnetism-Review article. *Geophysics*, 29: 482-516.
- Regan, R. D., and Rodriguez, P., 1981. An overview of the external magnetic field with regard to magnetic surveys. *Geophysical Surveys*, 4: 255-296.

- Saemundsson, K., 1970. Interglacial lava flows in the lowlands of southern Iceland and the problem of the two-tiered columnar jointing. *Jokull*, 20: 62-76.
- Sharma, P. V., 1976. *Geophysical Methods in Geology*. Elsevier scientific Publishing Co., Amsterdam, 428pp.
- Talwani, M., 1965. Computation with the help of a digital computer of magnetic anomalies caused by bodies of arbitrary shape. *Geophysics*, 30: 797-817.
- Talwani, M. and Heirtzler, J. R., 1964. Computation of magnetic anomalies caused by two dimensional structures of arbitrary shape, in *Computers in the mineral industries, part 1: Stanford University publications, Geol. Sciences*, 9: 464-480.
- Telford, W. M., Geldart, L. P., Sheriff, R. E. and Keys, D. A., 1976. *Applied Geophysics*. Cambridge University Press, Cambridge, 860pp.
- Vacquier, V., 1972. *Geomagnetism in Marine Geology*. Elsevier Oceanography Series-6, Elsevier, Amsterdam, 185pp.
- Vacquier, V., Steenland, N. C., Henderson, R. G., and Zietz, I., 1951. Interpretation of aeromagnetic maps. *Geol. Soc. Am. Mem.*, 47: 151pp.